Physics Letters A 377 (2013) 1837–1843

Contents lists available at SciVerse ScienceDirect

Physics Letters A

www.elsevier.com/locate/pla

Quantum Zeno and anti-Zeno effects measured by transition probabilities

Wenxian Zhang [a,b,c,d,*], A.G. Kofman [c,e], Jun Zhuang [b], J.Q. You [g,f,c], Franco Nori [c,e]

[a] School of Physics and Technology, Wuhan University, Wuhan, Hubei 430072, China
[b] Department of Optical Science and Engineering, Fudan University, Shanghai 200433, China
[c] CEMS, RIKEN, Saitama 351-0198, Japan
[d] Kavli Institute for Theoretical Physics China, CAS, Beijing 100190, China
[e] Department of Physics, The University of Michigan, Ann Arbor, MI 48109-1040, USA
[f] Department of Physics, Fudan University, Shanghai 200433, China
[g] Beijing Computational Science Research Center, Beijing 10084, China

ARTICLE INFO

Article history:
Received 7 October 2012
Received in revised form 4 May 2013
Accepted 14 May 2013
Available online 16 May 2013
Communicated by P.R. Holland

Keywords:
Quantum Zeno effect
Dynamical decoupling
Decay freezing

ABSTRACT

Using numerical calculations, we compare the transition probabilities of many spins in random magnetic fields, subject to either frequent projective measurements, frequent phase modulations, or a mix of modulations and measurements. For various distribution functions, we find the transition probability under frequent modulations is suppressed most if the pulse delay is short and the evolution time is larger than a critical value. Furthermore, decay freezing occurs only under frequent modulations as the pulse delay approaches zero. In the large pulse-delay region, however, the transition probabilities under frequent modulations are highest among the three control methods.

1. Introduction

Quantum coherence is of key importance in studying microscopic and mesoscopic quantum systems and in developing quantum devices, including quantum registers in quantum computing [1–5] and spintronic devices [6]. Many methods have been developed to extend the coherence time of a quantum system, particularly those methods using the quantum Zeno effect via either frequent measurements or frequent modulations [7–10].

Utilizing the quantum Zeno effect, the coherence time of a quantum system can be extended significantly in nuclear and electron spin systems [11–16], trapped ions [17,18], ultracold atomic Bose–Einstein condensates [19,20], and other physical systems [21–32]. Two frequent (periodic) control methods are often employed: either projective measurements or strong modulations. A systematic comparison of these two methods was made by Facchi et al. [33]: By calculating the transition rates, they compared the quantum Zeno/anti-Zeno effect in a two-level system via three methods: either (i) frequent measurements, (ii) frequent modulations, or (iii) a strong coupling to an auxiliary state. They assumed in the Markovian approximation that the controlled survival probabilities of an initial state p_s have always an exponential form and thus a well-defined transition rate γ_c for short times, i.e., $p_s(t) = e^{-\gamma_c t}$.

Zhang et al. [34–36], however, found that some systems exhibit decay freezing (exactly zero "transition rate"), where the transition probability becomes a constant after many modulation periods if the pulse delay is short, $p(t > t_s) \equiv p(t_s)$. Experimental evidence of decay freezing has also been shown in donor spins under dynamical decoupling pulse sequences [37,38]. In these cases, the exponential form assumed in Ref. [33] is invalid due to the violation of the Markovian approximation. Therefore, it is of particular interest to directly compare in the same system the transition probabilities, instead of the transition rates, under either frequent measurements or frequent modulations (see Fig. 1).

In this Letter, we revisit the study of the transitions of many spins in random magnetic fields under either frequent measurements or frequent modulations. The spins will be assumed to be initially in their spin-up state. Using exact numerical calculations, we systematically compare the performance of the three control methods in suppressing/enhancing the transition probabilities for three distributions (Gaussian, Lorentzian, and exponential) of the random local fields.

This Letter is organized as follows. In Section 2 we formulate the spin system's free dynamics and controlled dynamics under either (i) frequent measurements, (ii) frequent modulations, or (iii) a mix of modulations and measurements. We present numerical

* Corresponding author at: School of Physics and Technology, Wuhan University, Wuhan, Hubei 430072, China. Tel.: +86 27 68753517.
E-mail address: wxzhang@whu.edu.cn (W. Zhang).

0375-9601/$ – see front matter
http://dx.doi.org/10.1016/j.physleta.2013.05.029

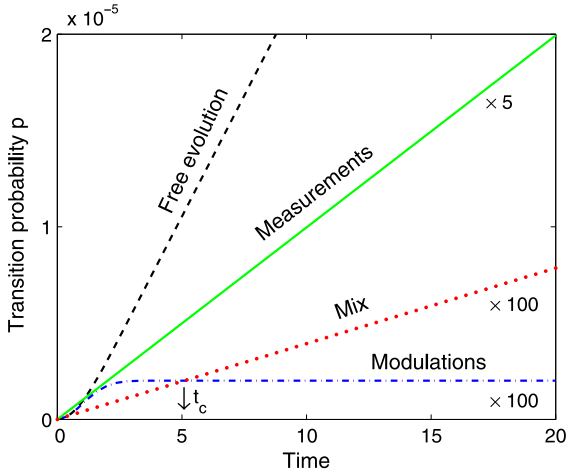

Fig. 1. (Color online.) Comparison of transition probabilities p for free evolution (dashed line), under frequent measurements (solid line, multiplied by 5), under frequent modulations (dash-dotted line, multiplied by 100. Presented data are for even-number modulation pulses), and under a mix of measurements and modulations (dotted line, multiplied by 100). Here the distribution has a Gaussian form [see Eq. (18)] with $\omega_m = 0$ and $\Gamma = 1$. The pulse delay is $\tau = 0.2$. The tiny arrow marks the critical time t_c where the transition probabilities are the same under the modulations and under the mix of modulations and measurements. Frequent measurements and the mix method suppress the transition rate while frequent modulations freeze the transition probability.

results in Section 3 for the three magnetic field distributions and compare in detail the performance of the three control methods listed above. Conclusions and discussions are presented in Section 4.

2. Evolution of the system

We consider K spin-1/2 particles in random longitudinal (z) magnetic fields, but spatially uniform horizontal (x) fields [39]:

$$H = \sum_{k=1}^{K} \frac{\omega_k}{2}\sigma_{kz} + g\sum_{k=1}^{K}\sigma_{kx}, \tag{1}$$

where k is the spin index, and σ_{kz} and σ_{kx} are the Pauli matrices for the kth spin. Also, ω_k and $2g$ are the Zeeman splitting of the kth spin along the longitudinal and transverse direction, respectively. We assume that single-spin operations and detection are not accessible, but the ensemble ones are available, which is the case in nuclear spin experiments. We also assume that g is much smaller than the typical value of ω_k, i.e., $b \gg g$ with $b \equiv (\sum_k \omega_k^2/K)^{1/2}$.

2.1. Free evolution

By initially setting all spins in the spin-up state, the transition probability to the spin-down state becomes

$$p_0(t) = \frac{1}{K}\sum_{k=1}^{K}\frac{g^2}{\Omega_k^2}\sin^2\Omega_k t \tag{2}$$

with $\Omega_k^2 = (\omega_k/2)^2 + g^2$. This result is exact. Note that this transition probability is nothing but the difference between 1 and the average polarization of the many-spin system m, i.e., $p_0 = 1 - m$. For a freely evolving system, m shows an exponential decay with a decay rate proportional to g^2. If the distribution of ω_k is dense, we can replace the sum over k with an integral over ω, i.e.,

$$\lim_{K\to\infty}\frac{1}{K}\sum_k [\,] = \int_{-\omega_c}^{\omega_c} d\omega\,[\,]\rho(\omega)$$

where $\rho(\omega) = (1/K)(dk/d\omega)$ is the density of "mode" [40] and $\omega_c = \max(|\omega_k|/2)$. Then

$$p_0(t) \approx \int d\omega\,\rho(\omega)\frac{g^2}{\Omega^2}\sin^2\Omega t,$$

where $\rho(\omega)$ is the distribution ("mode" density) function and is normalized: $\int d\omega\,\rho(\omega) = 1$. In this short time region, $\Gamma^{-1} \ll t \ll |g|^{-1}$, with Γ being the spectrum width ($\Gamma = \int d\omega\,\rho(\omega)(\omega - \langle\omega\rangle)^2$ and $\langle\omega\rangle = \int d\omega\,\rho(\omega)\omega$), the integrand $\sin^2\Omega t/\Omega^2$ sharply peaks at $\Omega \approx 0$. For a flat distribution function $\rho(\omega)$, the transition probability becomes

$$\begin{aligned} p_0(t) &\approx g^2\rho(0)\int d\omega\,\frac{\sin^2\Omega t}{\Omega^2} \\ &= 2\pi g^2\rho(0)t. \end{aligned} \tag{3}$$

A transition rate $\gamma_0 \equiv dp_0/dt = 2\pi g^2\rho(0)$ is then well defined.

Alternatively, from Eq. (2), the transition rate γ_0 to the spin-down state is given by

$$\gamma_0 \equiv \frac{dp_0}{dt} = \frac{g^2}{K}\sum_{k=1}^{K}\frac{\sin 2\Omega_k t}{\Omega_k}.$$

The above definition of the transition rate γ_0 agrees with the well-known one through $p_0(t) = 1 - e^{-\gamma_0 t}$ if $\gamma_0 t \ll 1$. Note that this transition rate γ_0 becomes constant if t is long enough (but still satisfies $t \ll |g|^{-1}$). Moreover, the transition probability $p_0(t)$ is still small for large enough t. In the dense-distribution approximation, the above equation for γ_0 becomes

$$\begin{aligned} \gamma_0 &\approx 2\pi g^2\int d\omega\,\rho(\omega)\delta(\omega) \\ &= 2\pi g^2\rho(0) \end{aligned} \tag{4}$$

which is consistent with the result of Eq. (3).

2.2. Controlled evolution under frequent modulations

The evolution of two-level systems under many phase-modulation control pulses has been widely investigated [41,26,42,43,33,44,12,36,45,46]. The control pulses are usually assumed to be hard, collective, and instantaneous [47]. We denote such a pulse as a Z pulse. For each spin under the Z pulse, the phase of the spin-down state is changed by π while the phase of the spin-up state is unchanged. Such a unitary transformation can be described by the rotation operator: $Z = \exp[i(\pi/2)\sum_k \sigma_{kz}] = \bigotimes_k(|\uparrow\rangle\langle\uparrow| - |\downarrow\rangle\langle\downarrow|)_k$. We have here neglected the constant $i = \sqrt{-1}$ which does not affect the conclusion. Since each spin evolves independently, the time evolution operator for an arbitrary spin after N pulses is [36]

$$U(t = N\tau) = (ZU_0)^N = \begin{pmatrix} U_{11} & U_{12} \\ -U_{21} & -U_{22} \end{pmatrix}^N, \tag{5}$$

where

$$U_{11} = U_{22}^* = \cos\Omega_k\tau - i\frac{\omega_k}{2\Omega_k}\sin\Omega_k\tau,$$

$$U_{12} = U_{21} = i\frac{g}{\Omega_k}\sin\Omega_k\tau$$

with τ being the delay between pulses. After a straightforward simplification (see Appendix A for a brief derivation), we obtain the controlled-evolution of the transition probability from the spin-up state to the spin-down state at time $t = N\tau$

$$p_{\rm mod}(t) = \frac{1}{K}\sum_{k=1}^{K}\frac{g^2}{\Omega_k^2}\sin^2\Omega_k\tau\frac{\sin^2 N\lambda_k}{\sin^2\lambda_k} \approx \int d\omega\,\rho(\omega)\frac{g^2}{\Omega^2}\sin^2\Omega\tau\frac{\sin^2 N\lambda}{\sin^2\lambda}, \quad (6)$$

where λ_k is determined by $\sin^2\lambda_k = 1-(\omega_k/2\Omega_k)^2\sin^2\Omega_k\tau$.

In the limit of short delay τ between pulses, $\tau\to 0$, the terms $\sin^2\lambda_k\approx 1$ and $\sin^2\Omega_k\tau\approx\Omega_k^2\tau^2$ to the leading order. For a large N, the term $\sin^2 N\lambda_k$ oscillates rapidly around its average $1/2$. Thus, the modulated transition probability $p_{\rm mod}$ in Eq. (6) becomes, after the integration over ω,

$$p_{\rm mod} \approx \frac{1}{2}\int d\omega\,\rho(\omega)\frac{g^2}{\Omega^2}\sin^2\Omega\tau \approx \frac{1}{2}g^2\tau^2, \quad (7)$$

which is nothing but half of the transition probability in the first delay τ [36]. In the derivation, we have used $(1/\Omega^2)\sin^2\Omega\tau\approx\tau^2$ if $\tau\ll\Omega^{-1}$ and $\int d\omega\,\rho(\omega)=1$. In this limiting case, $p_{\rm mod}$ becomes independent of the total evolution time and decay freezing occurs.

2.3. Controlled evolution under frequent measurements

We now assume that the measurements of the spin system are projective and periodic. The effect of such a measurement on the spin system is described by the projection operator, $\mathcal{P}=\bigotimes_k(|\uparrow\rangle\langle\uparrow|)_k$. By including the free evolution of the system during the measurement delay τ, we obtain the total evolution operator in a period for a single spin as

$$V\equiv\mathcal{P}U_0 = \begin{pmatrix} U_{11} & U_{12}\\ 0 & 0\end{pmatrix}. \quad (8)$$

Note that this evolution is nonunitary because of the measurement. It is straightforward to find that for N periods the evolution operator is

$$V^N = \begin{pmatrix} U_{11}^N & U_{12}U_{11}^{N-1}\\ 0 & 0\end{pmatrix}. \quad (9)$$

The survival probability of an initially spin-up state for the kth spin becomes

$$p_{k,s} = |U_{11}^N|^2 = \left[1-\left(\frac{g^2}{\Omega_k^2}\right)\sin^2\Omega_k\tau\right]^N. \quad (10)$$

By including all spins, the above Eq. (10) becomes

$$p_s(t=N\tau) = \frac{1}{K}\sum_{k=1}^{K}\left[1-\left(\frac{g^2}{\Omega_k^2}\right)\sin^2\Omega_k\tau\right]^N. \quad (11)$$

Under the dense-distribution approximation

$$p_s(t) \approx \int d\omega\,\rho(\omega)\left[1-\left(\frac{g^2}{\Omega^2}\right)\sin^2\Omega\tau\right]^N. \quad (12)$$

As a result, the total transition probability away from the initial spin-up state becomes

$$p_{\rm meas}(t) = 1-p_s(t). \quad (13)$$

In the limit $\tau\to 0$, the transition probability in Eq. (13) approaches

$$p_{\rm meas}(t) \approx 1-\int d\omega\,\rho(\omega)\left(1-g^2\tau^2\right)^N \approx g^2\tau^2 N \approx \gamma_{\rm meas}t \quad (14)$$

Table 1
Transition probabilities at $t=N\tau$ for three control methods (modulations, measurements, and mix) in the limit $\tau\to 0$ and $N\gg 1$.

Modulations	Measurements	Mix
$p_{\rm mod}=(1/2)g^2\tau^2$	$p_{\rm meas}=g^2\tau^2 N$	$p_{\rm mix}=(1/2)b^2g^2\tau^4 N$

with the transition rate $\gamma_{\rm meas}=g^2\tau$ and $t=N\tau$. Compared to the modulated case Eq. (7), where the transition rate is zero, Eq. (14) gives a *nonzero* transition rate $\gamma_{\rm meas}$, unless τ is exactly zero. In this sense, as long as the number of pulses is large, the transition probability under frequent measurements $p_{\rm meas}$ would always exceed that under frequent modulations (see Fig. 1).

2.4. Controlled evolution under a mix of modulations and measurements

By combining both frequent modulations and frequent measurements, we may utilize the advantages of both control methods. Here, a mixed cycle with a period of 2τ involves a modulation followed by a measurement. The nonunitary evolution operator for the cycle becomes

$$PU_0ZU_0 = \begin{pmatrix} U_{11}^2-U_{12}U_{21} & U_{12}(U_{11}-U_{22})\\ 0 & 0\end{pmatrix}. \quad (15)$$

The total survival probability of an initial spin-up state at time $t=N\tau$ is

$$p_s(t) = \frac{1}{K}\sum_{k=1}^{K}\left(1-\frac{\omega_k^2g^2}{\Omega_k^4}\sin^4\Omega_k\tau\right)^{N/2}.$$

It is easy to obtain the transition probability

$$p_{\rm mix} = 1-\frac{1}{K}\sum_{k=1}^{K}\left(1-\frac{\omega_k^2g^2}{\Omega_k^4}\sin^4\Omega_k\tau\right)^{N/2} \approx 1-\int d\omega\,\rho(\omega)\left(1-\frac{\omega^2g^2}{\Omega^4}\sin^4\Omega\tau\right)^{N/2}. \quad (16)$$

As seen from Eq. (16), it is difficult to obtain any analytical result in this case without specific information on the distribution function $\rho(\omega)$.

In the limit case $\tau\to 0$, the transition probability becomes

$$p_{\rm mix}\approx\gamma_{\rm mix}t \quad (17)$$

where $\gamma_{\rm mix}=(1/2)b^2g^2\tau^3$. When $t<t_c$, the mixed transition probability $p_{\rm mix}$ is smaller than the modulated transition probability $p_{\rm mod}$. The critical time t_c is

$$t_c = \left(b^2\tau\right)^{-1}.$$

This advantage of the mix method, for short times, is shown in Fig. 1. Of course, after many pulses, the transition rate of the mix method is nonzero, while that of the modulation method is zero. Thus, $p_{\rm mix}>p_{\rm mod}$ eventually when $t>t_c$.

As a summary, in Table 1 we list the results for the short-τ limit for the three control methods.

3. Numerical results

Given an arbitrary τ, we have to resort to numerical calculations in order to compare the transition probabilities in Eqs. (6), (13), and (16), except in the limiting case $\tau\to 0$. Among many forms of distribution functions $\rho(\omega)$, we consider three popular choices: Gaussian, Lorentzian, and exponential [9,48,36].

The Gaussian distribution function used here has the form:

$$\rho(\omega) = C \exp\left[-\frac{(\omega-\omega_m)^2}{2\Gamma^2}\right], \tag{18}$$

where C is the normalization constant, ω_m the peak position, and Γ the spectral width. In the numerical calculations, the lower and upper cutoff frequencies used here are $-\omega_c$ and ω_c, respectively, with $\omega_c = 100\Gamma$ for the three distributions.

The Lorentzian distribution function used here has the standard form:

$$\rho(\omega) = \frac{C}{(\omega-\omega_m)^2+\Gamma^2}. \tag{19}$$

The exponential distribution function used is

$$\rho(\omega) = C \exp\left[-\frac{|\omega-\omega_m|}{\Gamma}\right]. \tag{20}$$

There are many ways to compare the performance of the three control methods. We employ two ways to compare the transition probabilities of the spin system: (a) For $N = 2$ pulses, we vary the pulse delay τ to investigate the dependence of the performance of the control method on the pulse delay; (b) We fix the total evolution time $t = N\tau$ by varying the number of pulses (accordingly the pulse delay τ) to investigate the dependence on the number of pulses.

3.1. Comparison of two-pulse results with different pulse delays

As a starting point, let us compare two-pulse effects via either modulations, measurements, or the mix of a modulation followed by a measurement. It is easy to find that the transition probability subject to two modulations is

$$p_{\rm mod} = \int d\omega\, \rho(\omega) \frac{g^2\omega^2}{\Omega^4} \sin^4 \Omega\tau \tag{21}$$

and that under two measurements

$$p_{\rm meas} = \int d\omega\, \rho(\omega) \frac{g^2}{\Omega^2} \sin^2 \Omega\tau \left(2 - \frac{g^2}{\Omega^2}\sin^2\Omega\tau\right). \tag{22}$$

The mix of one modulation and one measurement is exactly the same as two modulations, $p_{\rm mix} = p_{\rm mod}$.

We plot the two-pulse transition probabilities in Fig. 2 for Gaussian, Lorentzian, and exponential distributions. For the cases of $\omega_m = 0$, the top row of Fig. 2 shows that both modulations and measurements suppress the transition probability (quantum Zeno effect), compared to the free-evolution case. In addition, the transition probabilities under two modulations $p_{\rm mod}$ are *always smaller* than those under two measurements $p_{\rm meas}$, $p_{\rm mod} < p_{\rm meas}$. While for the cases of $\omega_m = 2\Gamma$, both methods (i.e., two measurements or two modulations) also suppress the transition probability and $p_{\rm mod} < p_{\rm meas}$, if τ is small, but the two methods enhance the transition probability (quantum anti-Zeno effect) and $p_{\rm mod} > p_{\rm meas}$, if τ is large. The cross $p_{\rm mod} = p_{\rm meas}$ occurs around $\tau \approx 1$ in Fig. 2. In the limit of extremely small τ, i.e., $\tau \ll \Gamma^{-1}$,

$$p_0 \approx \int d\omega\, \rho(\omega) \frac{g^2}{\Omega^2} \sin^2 2\Omega\tau \approx 4g^2\tau^2.$$

Similarly,

$$p_{\rm mod} \approx g^2\tau^4 \int d\omega\, \rho(\omega)\omega^2 = g^2 b^2 \tau^4,$$

$$p_{\rm meas} \approx 2g^2\tau^2.$$

So we find that $p_{\rm mod}/p_0 \to 0$ and $p_{\rm meas}/p_0 \to 1/2$, which agrees well with numerical results shown in Fig. 2 for all the considered cases. But in the limit of large τ, we find that both controlled transition probabilities approach the transition probability of free evolution, i.e., the control pulses have little effect on the evolution of the system. It is interesting that all three distributions show consistent and similar results.

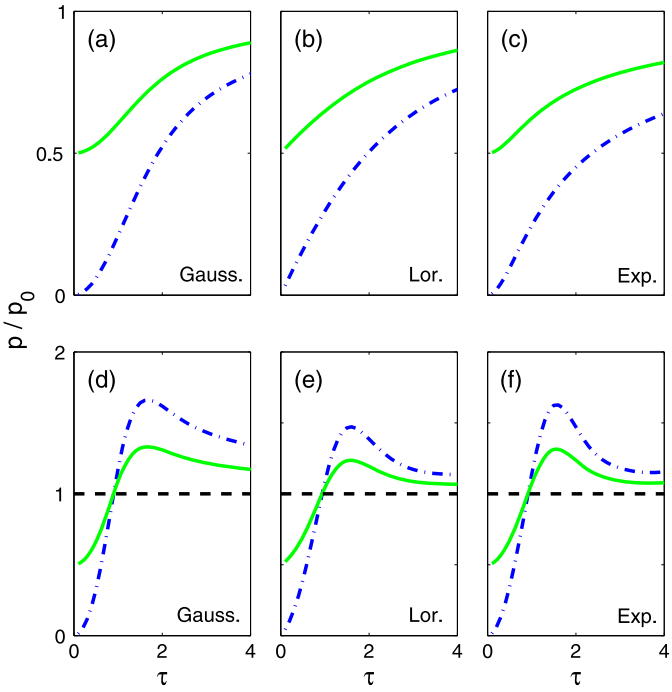

Fig. 2. (Color online.) Transition probabilities (scaled by the free-evolution transition probability) of a many-spin system under two measurements (green solid lines) or two modulations (blue dash-dotted lines) for three distribution functions: Left column [(a) and (d)], Gaussian; Middle column [(b) and (e)], Lorentzian; Right column [(c) and (f)], exponential. The horizontal black dashed lines in the panels (d), (e), (f) of the bottom row mark the boundary between quantum Zeno and quantum anti-Zeno effect. The peaks of the distributions are chosen as $\omega_m = 0$ for the top row of panels [(a), (b), and (c)] and $\omega_m = 2\Gamma$ for the bottom row [(d), (e), and (f)], respectively. The parameters $\Gamma = 1$ and $g = 0.001$ are used for all cases. Hereafter, time is measured in units of Γ^{-1}. The transition probabilities under two modulations are smaller than those under measurements for *all* τs, if $\omega_m = 0$ (top panels), and for *small* τs, if $\omega_m = 2\Gamma$ (bottom panels).

3.2. Comparison of multi-pulse results at fixed evolution time

Next we consider the cases of varying N pulses but a fixed total evolution time $t = N\tau$, i.e., τ varies as t/N. We choose $t = 10$, which satisfies $\Gamma t \gg 1$. By changing N from 1 to 100, the pulse delay τ decreases from 10 to 0.1 and $\Gamma\tau \in [0.1, 10]$ correspondingly, sweeping from a value much larger than 1 to a value much less than 1. Under these conditions, both the quantum Zeno effect and the anti-Zeno effect may appear.

The transition probabilities of the spin system for Gaussian, Lorentzian, and exponential distributions are shown in Fig. 3. Again, we scale the transition probabilities under measurements, modulations, or the mix of modulations and measurements, by dividing the transition probability of the free evolution at the same time. In the top row of Fig. 3, where $\omega_m = 0$, the transition probabilities under frequent modulations are smaller than those under frequent measurements and the probabilities for the mix method lie in between, i.e., $p_{\rm mod} < p_{\rm mix} < p_{\rm meas}$. In addition, $p_{\rm mod,meas,mix} < p_0$ for all N, showing that frequent modulations, frequent measurements, and the mix method all suppress the transition probability and only the quantum Zeno effect occurs.

The bottom row of Fig. 3, where $\omega_m = 2\Gamma$, shows a more complex phenomenon:

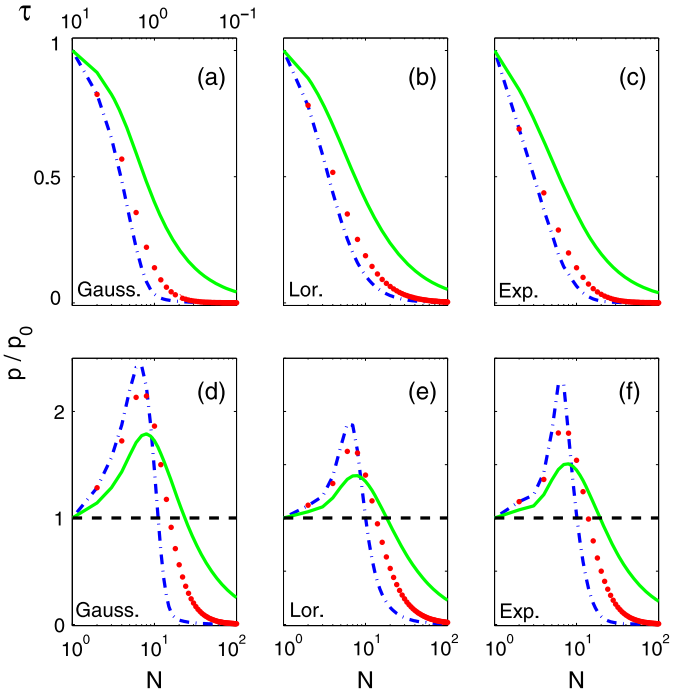

Fig. 3. (Color online.) Quantum Zeno effect and anti-Zero effect in controlling the transition probabilities with frequent measurements (green solid lines), frequent modulations (blue dash-dotted lines), and the mix of modulations and measurements (red dotted lines). The transition probabilities subject to control pulses are normalized by dividing the free-evolution transition probability for the same time. The horizontal black dashed lines in the panels (d), (e), (f) of the bottom row mark the boundary between quantum Zeno and quantum anti-Zeno effect. The distribution functions are Gaussian [left column, (a) and (d)], Lorentzian [middle column, (b) and (e)], and exponential [right column, (c) and (f)]. In the top and the bottom row, $\omega_m = 0$ and 2Γ, respectively. The total evolution time $t = N\tau = 10$ is fixed. Other parameters are the same as in Fig. 2. In the top row, the modulation method outperforms the measurement one in suppressing the transition probability of the spin system. While in the bottom row, the modulation method is worse than the measurement one if the number of pulses N is small, but better if N is large.

1. For small N, the quantum anti-Zeno effect $p_{\mathrm{mod,meas,mix}} > p_0$ appears (i.e., the enhancement of the transition probabilities) for all control methods.
2. For large N, the quantum Zeno effect $p_{\mathrm{mod,meas,mix}} < p_0$ (i.e., the suppression of the transition probabilities) appears for all control methods.
3. For the same value of N, by comparing the performance of the modulation, the measurement, and the mix methods, we find $p_{\mathrm{mod}} > p_{\mathrm{mix}} > p_{\mathrm{meas}}$ for small N but $p_{\mathrm{mod}} < p_{\mathrm{mix}} < p_{\mathrm{meas}}$ for large N.
4. All three methods intersect around $N = 10$ (or $\tau = 1$), where $p_{\mathrm{mod}} \approx p_{\mathrm{meas}} \approx p_{\mathrm{mix}}$.

For extremely small τ (large N), which is outside the region shown in Fig. 3, the mix method performs better than the modulation method (see Fig. 1). For a given fixed total time t, by setting $p_{\mathrm{mix}} = p_{\mathrm{mod}}$ and using the formula listed in Table 1, we find that the critical value of τ is

$$\tau_c = \frac{1}{b^2 t}.$$

Correspondingly, the critical number of pulses is

$$N_c = t/\tau_c = b^2 t^2.$$

We remark here that the above conclusions on the performance order of the quantum Zeno and anti-Zeno effects agree with results obtained with other analytical methods in the Markovian approximation [33], for instance, the modulation method is the best at suppressing the transition. But we do not assume any specific decay form of the transition probability while an exponential form is assumed in Refs. [42,33]. In fact, an exponential decay form is not always the case, especially with the modulation method (see Fig. 1). Our results of transition probability may be valid in a wider parameter region.

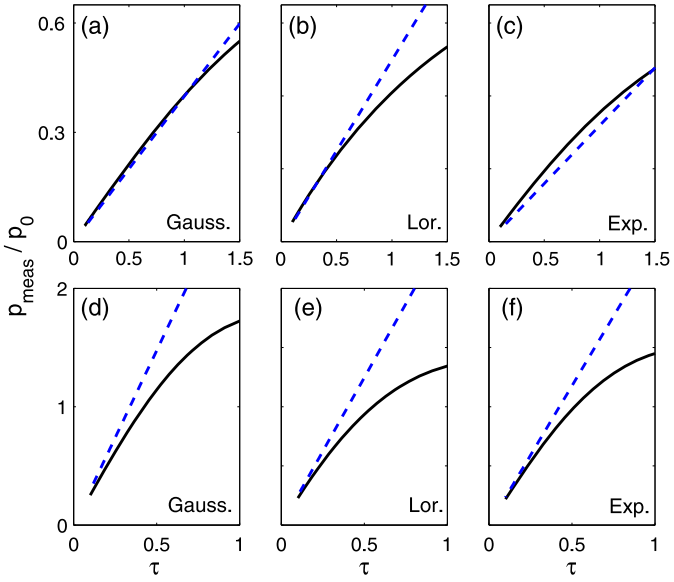

Fig. 4. (Color online.) Transition probability of the spin system under frequent measurements at the fixed time $t = 10$ for different short pulse delays τ (black solid line). The distributions are Gaussian (left column), Lorentzian (middle column), and exponential (right column). Also, we use $\omega_m = 0$ (top row) and $\omega_m = 2\Gamma$ (bottom row). The blue dashed lines are obtained from Eq. (27).

3.3. Short τ limit at fixed time

Noticing that all the curves for different distribution functions in Fig. 3 give similar tails at large N (small τ), we next compare how the controlled system approaches its limiting case $\tau \to 0$. We note here the difference between cases in this section and the cases in Section 3.1, where $t = 2\tau \to 0$ if $\tau \to 0$. For the free evolution, the transition probability of the spin system can be approximated as follows if $\Gamma^{-1} \ll t \ll \gamma_0^{-1}$

$$p_0 \approx \gamma_0 t \tag{23}$$

with $\gamma_0 = 2\pi g^2 \rho(0)$ being the transition rate. Similarly, the transition probability under frequent measurements [see Eq. (14)] at times $t \ll \gamma_{\mathrm{meas}}^{-1}$ is

$$p_{\mathrm{meas}} \approx \gamma_{\mathrm{meas}} t. \tag{24}$$

The above equation shows that the transition rate $\gamma_{\mathrm{meas}} = g^2\tau$ can be defined. Compared to the case of free evolution, this rate γ_{meas} is independent of the distribution function and depends linearly on the pulse delay τ.

Quite differently, the transition probability [see Eq. (7)] under frequent modulations is frozen for small τ,

$$p_{\mathrm{mod}} \approx \frac{1}{2} g^2 \tau^2. \tag{25}$$

Obviously, no decay rate can be defined. It is remarkable that this transition probability is independent of the total evolution time and the distribution function. Decoherence is frozen after several control pulses if τ is small [34,36,49]. This transition freezing effect shown in Eq. (25) has been demonstrated experimentally in Refs. [37,38].

Under the mix control method, the transition probability grows linearly

$$p_{\mathrm{mix}} \approx \gamma_{\mathrm{mix}} t \tag{26}$$

with a well-defined transition rate $\gamma_{\mathrm{mix}} = b^2 g^2 \tau^3$ in the limit $\tau \to 0$. Note that this transition rate depends on the distribution function since $b^2 = \int d\omega\, \omega^2 \rho(\omega)$.

In the small τ limit, it is easy to obtain

$$\frac{p_{\mathrm{meas}}}{p_0} \approx \frac{\tau}{2\pi\rho(0)},$$
$$\frac{p_{\mathrm{mix}}}{p_0} \approx \frac{b^2\tau^3}{2\pi\rho(0)}. \tag{27}$$

We numerically check the relationship for frequent measurements by redrawing the large-N results of Fig. 3 and using τ as the horizontal axis. Fig. 4 shows how the above limiting results are approached for different distributions as τ approaches zero.

4. Conclusion and discussion

In summary, using numerical calculations, we compare the transition probabilities of a many-spin system in local random fields (with Gaussian, Lorentzian, or exponential distributions) under either frequent modulations, frequent projective measurements, or the mix of modulations and measurements. In the small-τ region, all three control methods suppress the transition probability of the system. Among the three control methods, the modulation one exhibits the largest suppression of the transition probability if the total evolution time is larger than the critical time, and the transition freezes after many modulation pulses. If the time is smaller than the critical time, the mix method is the most effective at suppressing the transition probabilities.

In the large τ region, all three control methods also suppress the transition probability if $\omega_m = 0$, but enhance the transition probability if ω_m is large. Overall, the modulation method changes more drastically the dynamics of the system [26]: The modulation method outperforms the other two methods in either suppressing the transition in the small τ region or enhancing the transition in the large τ region, provided that the evolution time is larger than the critical time t_c.

The modulation-pulse delay is the same in all of our calculations. By adopting varying pulse delay, such as concatenation or Uhrig's protocol [27,28], we could in principle suppress/enhance much more the transition probability. We believe that the transition probability would deviate more from an exponential decay under these more complicated modulation pulse sequences.

Acknowledgements

W.Z. is grateful for discussions with S. Ashhab, C.P. Sun, and S. Pascazio. W.Z. and J.Q.Y. acknowledge support by the National Basic Research Program of China under Grant No. 2009CB929300. W.Z. acknowledges support by the National Natural Science Foundation of China under Grant Nos. 10904017, 11275139, NCET, Specialized Research Fund for the Doctoral Program of Higher Education of China under Grant No. 20090071120013, and Shanghai Pujiang Program under Grant No. 10PJ1401300. F.N. acknowledges partial support from the Army Research Office, JSPS-RFBR Contract No. 12-02-92100, Grant-in-Aid for Scientific Research (S), MEXT Kakenhi on Quantum Cybernetics, and Funding Program for Innovative R&D on S&T (FIRST).

Appendix A. Derivation of Eq. (6)

Similar to the derivation in Ref. [36], it is easy to find with a diagonalization method that

$$U(t = N\tau) = \begin{pmatrix} A & B \\ C & D \end{pmatrix} \tag{A.1}$$

where

$$A = i^N \left(\cos N\lambda_k - i \cos \Omega_k \tau \frac{\sin N\lambda_k}{\sin \lambda_k} \right),$$
$$B = -i^N \frac{g}{\Omega_k} \sin \Omega_k \tau \frac{\sin N\lambda_k}{\sin \lambda_k},$$
$$C = i^N \frac{g}{\Omega_k} \sin \Omega_k \tau \frac{\sin N\lambda_k}{\sin \lambda_k},$$
$$D = i^N \left(\cos N\lambda_k + i \cos \Omega_k \tau \frac{\sin N\lambda_k}{\sin \lambda_k} \right).$$

The transition probability from an initial spin-up state to the spin-down state under frequent modulations is

$$p_{\mathrm{mod}} = \frac{1}{K} \sum_{k=1}^{K} \left| \langle \downarrow_k | U | \uparrow_k \rangle \right|^2 = \frac{1}{K} \sum_{k=1}^{K} |B|^2,$$

which is Eq. (6).

References

[1] M.A. Nielsen, I.L. Chuang, Quantum Computations and Quantum Information, Cambridge University Press, Cambridge, 2000.
[2] T.D. Ladd, F. Jelezko, R. Laflamme, Y. Nakamura, C. Monroe, J.L. O'Brien, Nature (London) 464 (2010) 45.
[3] J. Stolze, D. Suter, Quantum Computing, Wiley–VCH, Weinheim, 2008.
[4] W.P. Schleich, H. Walther, Elements of Quantum Information, Wiley–VCH, Weinheim, 2008.
[5] I. Buluta, S. Ashhab, F. Nori, Rep. Prog. Phys. 74 (2011) 104401.
[6] I. Zutic, J. Fabian, S. Das Sarma, Rev. Mod. Phys. 76 (2004) 323.
[7] B. Misra, E.C.G. Sudarshan, J. Math. Phys. 18 (1977) 756.
[8] R.J. Cook, Phys. Scr. T 21 (1988) 49.
[9] A.G. Kofman, G. Kurizki, Nature (London) 405 (2000) 546.
[10] P. Facchi, H. Nakazato, S. Pascazio, Phys. Rev. Lett. 86 (2001) 2699.
[11] U. Haeberlen, High Resolution NMR in Solids: Selective Averaging, Academic Press, New York, 1976.
[12] W. Zhang, V.V. Dobrovitski, L.F. Santos, L. Viola, B.N. Harmon, J. Mod. Opt. 54 (2007) 2629.
[13] B. Lee, W.M. Witzel, S.D. Sarma, Phys. Rev. Lett. 100 (2008) 160505.
[14] W. Yang, R.-B. Liu, Phys. Rev. Lett. 101 (2008) 180403.
[15] M.J. Biercuk, H. Uys, A.P. VanDevender, N. Shiga, W.M. Itano, J.J. Bollinger, Nature (London) 458 (2009) 996.
[16] J. Du, X. Rong, N. Zhao, Y. Wang, J. Yang, R.B. Liu, Nature (London) 461 (2009) 1265.
[17] W.M. Itano, D.J. Heinzen, J.J. Bollinger, D.J. Wineland, Phys. Rev. A 41 (1990) 2295.
[18] W.M. Itano, D.J. Heinzen, J.J. Bollinger, D.J. Wineland, Phys. Rev. A 43 (1991) 5168.
[19] E.W. Streed, J. Mun, M. Boyd, G.K. Campbell, P. Medley, W. Ketterle, D.E. Pritchard, Phys. Rev. Lett. 97 (2006) 260402.
[20] B.-Y. Ning, J. Zhuang, J.Q. You, W. Zhang, Phys. Rev. A 84 (2011) 013606.
[21] C. Search, P.R. Berman, Phys. Rev. Lett. 85 (2000) 2272.
[22] E. Frishman, M. Shapiro, Phys. Rev. Lett. 87 (2001) 253001.
[23] J. Evers, C.H. Keitel, Phys. Rev. Lett. 89 (2002) 163601.
[24] E. Frishman, M. Shapiro, Phys. Rev. A 68 (2003) 032717.
[25] M.C. Fischer, B. Gutiérrez-Medina, M.G. Raizen, Phys. Rev. Lett. 87 (2001) 040402.
[26] A.G. Kofman, G. Kurizki, Phys. Rev. Lett. 87 (2001) 270405.
[27] K. Khodjasteh, D.A. Lidar, Phys. Rev. Lett. 95 (2005) 180501.
[28] G.S. Uhrig, Phys. Rev. Lett. 98 (2007) 100504.
[29] X.-B. Wang, J.Q. You, F. Nori, Phys. Rev. A 77 (2008) 062339.
[30] L. Zhou, S. Yang, Y.-X. Liu, C.P. Sun, F. Nori, Phys. Rev. A 80 (2009) 062109.
[31] X. Cao, J.Q. You, H. Zheng, A.G. Kofman, F. Nori, Phys. Rev. A 82 (2010) 022119.
[32] X. Cao, Q. Ai, C.-P. Sun, F. Nori, Phys. Lett. A 376 (2012) 349.
[33] P. Facchi, S. Tasaki, S. Pascazio, H. Nakazato, A. Tokuse, D.A. Lidar, Phys. Rev. A 71 (2005) 022302.

[34] W. Zhang, V.V. Dobrovitski, L.F. Santos, L. Viola, B.N. Harmon, Phys. Rev. B 75 (2007) 201302(R).
[35] W. Zhang, N.P. Konstantinidis, V.V. Dobrovitski, B.N. Harmon, L.F. Santos, L. Viola, Phys. Rev. B 77 (2008) 125336.
[36] W. Zhang, J. Zhuang, Phys. Rev. A 79 (2009) 012310.
[37] A.M. Tyryshkin, Z.-H. Wang, W. Zhang, E.E. Haller, J.W. Ager, V.V. Dobrovitski, S.A. Lyon, arXiv:1011.1903v2 [quan-ph].
[38] Z.-H. Wang, W. Zhang, A.M. Tyryshkin, S.A. Lyon, J.W. Ager, E.E. Haller, V.V. Dobrovitski, Phys. Rev. B 85 (2012) 085206.
[39] C.P. Slichter, Principles of Magnetic Resonance, Springer-Verlag, New York, 1992.
[40] M.O. Scully, M.S. Zubairy, Quantum Optics, Cambridge University Press, Cambridge, 1997.
[41] A.G. Kofman, G. Kurizki, T. Opatrný, Phys. Rev. A 63 (2001) 042108.
[42] A.G. Kofman, G. Kurizki, Phys. Rev. Lett. 93 (2004) 130406.
[43] G.S. Agarwal, M.O. Scully, H. Walther, Phys. Rev. Lett. 86 (2001) 4271.
[44] I. Feranchuk, L. Komarov, A. Ulyanenkov, J. Phys. B 35 (2002) 3957.
[45] H. Zheng, S.Y. Zhu, M.S. Zubairy, Phys. Rev. Lett. 101 (2008) 200404.
[46] Q. Ai, Y. Li, H. Zheng, C.P. Sun, Phys. Rev. A 81 (2010) 042116.
[47] L. Viola, E. Knill, S. Lloyd, Phys. Rev. Lett. 82 (1999) 2417.
[48] G.S. Agarwal, M.O. Scully, H. Walther, Phys. Rev. A 63 (2001) 044101.
[49] R.-B. Liu, W. Yao, L.J. Sham, New J. Phys. 9 (2007) 226.